M. Hautakorpi, A. Shevchenko, and M. Kaivola. 2004. Spatially smooth evanescent-wave profiles in a multimode hollow optical fiber for atom guiding. Optics Communications, volume 237, numbers 1-3, pages 103-110.

Available online at www.sciencedirect.com
SCIENCE DIRECT®
Optics Communications 237 (2004) 103–110
OPTICS COMMUNICATIONS
www.elsevier.com/locate/optcom

Spatially smooth evanescent-wave profiles in a multimode hollow optical fiber for atom guiding

Markus Hautakorpi *, A. Shevchenko, M. Kaivola

Optics and Molecular Materials, Helsinki University of Technology, P.O. Box 2200, 02015 HUT, Finland

Received 27 January 2004; received in revised form 30 March 2004; accepted 31 March 2004

Abstract

We analyze two methods for obtaining a smooth evanescent-wave intensity profile on the inner surface of a multimode hollow optical fiber to be used as a waveguide for neutral atoms. The first method is based on the selective excitation of fiber modes with a laser beam possessing orbital angular momentum, of which Laguerre–Gaussian beams are considered as an example. The second method makes use of a rapid variation of the speckle pattern of the fiber's evanescent-wave in the timescale of the atomic motion. The variation is provided by dithering the angle of incidence of a Gaussian laser beam at the fiber entrance. The optimal beam waist and direction of dithering are determined.

PACS: 32.80.Pj; 39.25.+k; 03.75.Be

Keywords: Hollow optical fiber; Atom guiding; Orbital angular momentum of light; Speckle

1. Introduction

In recent years, hollow optical fibers (HOFs) have been studied extensively for their use as waveguides for neutral atoms. The operation of the waveguide is based on the repulsive dipole interaction between the atoms and a blue-detuned evanescent-wave on the fiber's inner surface [1,2]. The intensity of the evanescent-wave determines the largest allowed transverse velocity of atoms that can still be guided through the fiber by consecutive reflections from the evanescent-wave. HOFs have also found applications, for example, in studies of fundamental quantum phenomena in small cavities [3] and in the construction of fiber-based components, such as filters [4] and mode converters [5] in optical telecommunications.

In principle, a single-mode HOF would lend itself perfectly for guiding atoms, because the evanescent-wave distribution of the fundamental $LP_{0,1}$ mode is homogeneous over the fiber's inner surface. Furthermore, due to the small transverse dimensions of the core, which are typically on the order of a few optical wavelengths, the power of the mode is confined to a small transverse area [6].

* Corresponding author. Tel.: +358-9-451-2581; fax: +358-9-451-3155.
E-mail address: Markus.Hautakorpi@hut.fi (M. Hautakorpi).

0030-4018/$ - see front matter
doi:10.1016/j.optcom.2004.03.087

As a consequence, the intensity of the mode on the fiber's inner surface can be made high with a low-power laser. Unfortunately, the small opening of a single-mode HOF makes transfer of atoms into the waveguide inefficient. Moreover, it is difficult to couple light into the fiber core in such a way that the light would not prevent the atoms from getting into the fiber [7]. Injection of atoms into the fiber from the other end is also hampered by light, since the output field of the fiber is strongly concentrated in front of the fiber hole [8,9]. To our knowledge, guiding of atoms through single-mode HOFs has still not been demonstrated in practice.

By using multimode HOFs with larger transverse dimensions, these problems can be overcome. The incident-beam power can efficiently be coupled to propagating fiber modes, e.g., by directing a Gaussian laser beam to the rim of the fiber core. The fiber opening can then be made practically free of light. In addition, the output field of the majority of higher-order modes is dark along the fiber axis, which allows injection of atoms into the fiber from that end, too [8]. Thus, even for similar hole diameters, a multimode fiber can be loaded with atoms more efficiently than a single-mode fiber. A severe problem with the use of multimode HOFs is caused by the speckle, which originates from interference of the fiber modes. Consequently, there will be dark spots on the fiber's inner surface, to which the atoms can stick due to van der Waals interaction, or from which they can gain a high kinetic energy. The speckle has been one of the major factors that has reduced the flux of guided atoms through a multimode HOF in a number of experiments [10–12].

In this paper, we present two methods, by which the problem of speckle can be overcome in multimode HOFs. First, we propose a method of exciting a particular $\mathrm{LP}_{m,p}$ mode in a multimode HOF by using beams, which possess orbital angular momentum. Laguerre–Gaussian (LG_q^l) beams are considered as an example of such beams. With this method of excitation, the intensity distribution can be made homogeneous on the fiber's inner wall, and the output field of a higher-order mode, being dark on the axis, can be used in funneling atoms [8,13]. Second, we analyze a method of smoothing the speckle on the fiber's inner surface. The method, which was briefly described in [10], is based on rapid dithering of the angle of incidence of a Gaussian laser beam focused to the rim of the fiber core. The speckle grains on the fiber's inner wall will then move quickly and, if the dithering is performed fast enough, the atoms will only see a time-averaged, spatially smooth evanescent-wave intensity profile.

The paper is organized as follows: In Section 2, we present the method of calculating the excitation coefficients of individual fiber modes, when a laser beam is incident on the fiber facet. In Section 3, we determine the parameters of a number of incident LG_q^l beams, which can be used to make only one of the excitation coefficients to be nonzero. In Section 4, we characterize the time-averaged intensity profiles on the inner surface of the fiber resulting from the dithering of the incident angle of a Gaussian beam in two mutually orthogonal directions. We then describe the optimal way of carrying out the dithering. A discussion is presented in Section 5.

2. Theory

In this work, we consider weakly guiding fibers, in which the refractive index difference between the core and the cladding, $\Delta n = n_1 - n_2$, is small, typically less than one percent. The refractive index profile of a HOF is illustrated in Fig. 1, where $n_0 = 1$ is the refractive index of the hollow region and a and b are the inner and outer radius of the core, respectively. The thickness of the cladding is assumed to be infinite. The propagating $\mathrm{LP}_{m,p}$ modes of a weakly guiding HOF are linearly polarized in the plane perpendicular to the fiber axis. The scalar field of an $\mathrm{LP}_{m,p}$ mode can be written in cylindrical coordinates as [2] $E_{\mathrm{LP}}(r,\theta,z;t) = E_{m,p}(r,\theta)\exp(\mathrm{i}(\omega t - \beta_{m,p}z))$, where $E_{m,p}(r,\theta)$ is the amplitude and $\beta_{m,p}$ the propagation constant of the mode, and ω is the angular frequency of light. The mode amplitude $E_{m,p}$ can be written in the form [2]

$$E_{m,p}(r,\theta) = \begin{cases} AI_m(vr)\exp(-\mathrm{i}m\theta), & r \leqslant a, \\ [BJ_m(ur) + CN_m(ur)]\exp(-\mathrm{i}m\theta), & a < r < b, \\ DK_m(wr)\exp(-\mathrm{i}m\theta), & b \leqslant r. \end{cases} \tag{1}$$

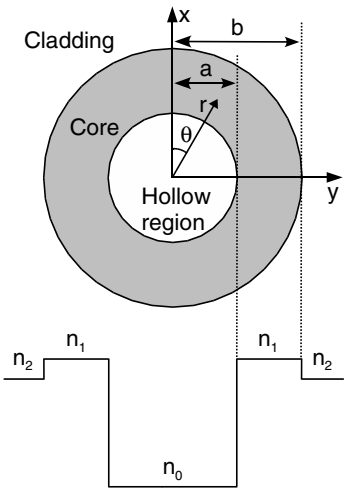

Fig. 1. Refractive index profile of a hollow optical fiber.

The boundary conditions at $r = a$ and $r = b$ relate the coefficients A, B, C and D to each other. These coefficients determine the power carried by the mode. The functions J_m and N_m are Bessel functions of the first and second kind of order m, respectively. Similarly, I_m and K_m denote modified Bessel functions of the first and second kind of order m, respectively. The parameters v, w and u are given by $v = \sqrt{\beta_{m,p}^2 - k^2 n_0^2}$, $w = \sqrt{\beta_{m,p}^2 - k^2 n_2^2}$, and $u = \sqrt{k^2 n_1^2 - \beta_{m,p}^2}$, with k denoting the wavenumber.

To describe the coupling of light to the fiber modes, we consider incident beams that belong to the family of Laguerre–Gaussian (LG_q^l) beams. The lowest-order beam LG_0^0 is an ordinary Gaussian beam. The higher-order LG_q^l beams with $l \neq 0$ possess orbital angular momentum [14], and they can be written in cylindrical coordinates (r', θ', z') as $E_{\mathrm{LG}}(r', \theta', z'; t) = E_{l,q}(r', \theta', z') \exp(\mathrm{i}(\omega t - kz'))$, where the amplitude $E_{l,q}$ is [15]

$$E_{l,q}(r', \theta', z') = A_{l,q} \frac{w_0}{W(z')} \left(\frac{r'}{W(z')} \right)^l L_q^l \left(\frac{2r'^2}{W^2(z')} \right) \times \exp(-r'^2/W^2(z')) \times \exp(-\mathrm{i}[l\theta' - (2q + l + 1)\arctan(z'/z_R) + kr'^2/2R(z')]). \quad (2)$$

Here, $A_{l,q}$ determines the power of the beam and the parameters W, R and z_R are given by $W(z') = w_0\sqrt{1 + z'^2/z_R^2}$, $R(z') = z' + z_R^2/z'$, and $z_R = w_0^2 k/2$. For the lowest-order beam LG_0^0 the parameter w_0 defines the beam waist and, as can be deduced from Eq. (2), it determines the radial extent of the higher-order beams as well. The parameter $R(z')$ defines the radius of curvature of the wavefront and the term $(2q + l + 1)\arctan(z'/z_R)$ is the Gouy phase. The function L_q^l is an associated Laguerre polynomial of the order q. If an LG_q^l beam is incident onto the fiber facet at a nonzero angle of incidence, its field distribution on the fiber facet can be obtained by using a Cartesian coordinate transformation

$$\begin{pmatrix} x' \\ y' \\ z' \end{pmatrix} = \begin{pmatrix} \cos\gamma & 0 & -\sin\gamma \\ -\sin\alpha\sin\gamma & \cos\alpha & -\sin\alpha\cos\gamma \\ \cos\alpha\sin\gamma & \sin\alpha & \cos\alpha\cos\gamma \end{pmatrix} \times \begin{pmatrix} x - x_0 \\ y - y_0 \\ z \end{pmatrix}, \quad (3)$$

where $(x_0, y_0, 0)$ is the position of the center of the beam, and the variables γ and α are the angles between the x and x' axes, and y and y' axes, respectively. The angle γ is assigned a value by rotation about the y' axis (parallel to the y axis) and the angle α by rotation about the new x' axis (see Fig. 2).

If the power carried by each individual $\mathrm{LP}_{m,p}$ mode of a HOF is normalized to unity by equating $\int\int |E_{m,p}(r, \theta)|^2 r\,\mathrm{d}r\,\mathrm{d}\theta$ to 1, the modes of the fiber

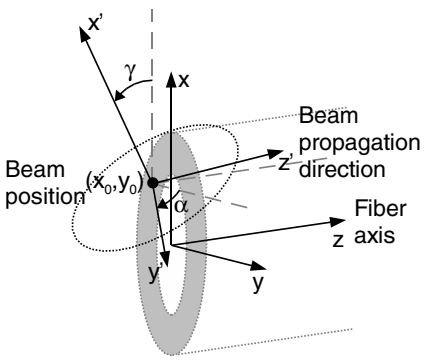

Fig. 2. Coordinate transformation. The first rotation takes place about the y' axis (parallel to the y axis) by an angle γ. The plane of the second rotation, about the x' axis by an angle α, is shown by dashed circle.

form a complete orthonormal basis. One can then expand an incident beam carrying unit power as

$$E_{l,q}(r',\theta',z') = \left(\sum_{m,p} C_{m,p}(\alpha,\gamma)E_{m,p}(r,\theta)\right) + E_{\mathrm{rad}} \tag{4}$$

with r', θ' and z' being expressed through Eq. (3). In Eq. (4), the excitation weights $C_{m,p}$ of the individual fiber modes are given by

$$C_{m,p}(\alpha,\gamma) = \int_0^{\infty}\int_0^{2\pi} [E_{m,p}(r,\theta)]^* E_{l,q}(r',\theta',z') r\,\mathrm{d}r\,\mathrm{d}\theta. \tag{5}$$

The overall contribution of the radiation modes is absorbed in the term E_{rad}. The reflection losses from the fiber facet are not considered. The fraction of power that is transferred to a specific $\mathrm{LP}_{m,p}$ mode is given by the value of $|C_{m,p}|^2$.

Far from the coupling plane, the contribution of the radiation modes can be neglected and the total field can be described by

$$E_{\mathrm{HOF}}(r,\theta,z;t) = \sum_{m,p} C_{m,p}(\alpha,\gamma)E_{m,p}(r,\theta) \times \exp(\mathrm{i}(\omega t - \beta_{m,p}z)). \tag{6}$$

The intensity distribution on the fiber's inner surface is obtained by calculating $|E_{\mathrm{HOF}}(a,\theta,z;t)|^2$.

3. Excitation of separate modes in a multimode HOF

The intensity of any single fiber mode $|E_{\mathrm{LP}}(r,\theta,z;t)|^2 = |E_{m,p}(r,\theta)|^2$ is independent of the coordinates θ and z (see Eq. (1)), i.e., the intensity distribution is homogeneous over the whole of the fiber's inner surface. If such a mode could be solely excited in the fiber, this would provide ideal conditions for atom guiding. In the following, we show how a Laguerre–Gaussian beam focused symmetrically onto the fiber entrance at normal incidence can be utilized for this purpose. The orbital angular momentum content of an LG_q^l beam is associated with the azimuthal field distribution $\exp(-\mathrm{i}l\theta')$ in Eq. (2) [14]. Similarly, the azimuthal dependence $\exp(-\mathrm{i}m\theta)$ of a fiber mode in Eq. (1) can also be associated with the orbital angular momentum of the guided mode. For such field distributions, in the coupling configuration described above, the azimuthal part of the excitation coefficients of Eq. (5) yields

$$C_{m,p} \propto \int_0^{2\pi} \exp(\mathrm{i}(m-l)\theta)\,\mathrm{d}\theta, \tag{7}$$

where we have used Eq. (2) at $z' = z = 0$. Equation (7) shows that the coefficients $C_{m,p}$ are nonzero only when the indices m and l are the same, i.e., when the orbital angular momentum content of the incident beam coincides with that of the guided mode. The magnitude of $|C_{m,p}|^2$ is then determined by the radial field distributions of the overlapping fields. Note that one cannot obtain an azimuthally homogeneous intensity distribution by simply adjusting the incident angle of an ordinary Gaussian beam in order to excite the higher-order modes. Unavoidably then, several modes of the form of Eq. (1) would be excited. In particular, the presence of modes with opposite signs of m with comparable amplitudes will give rise to sinusoidal azimuthal modulation of the field, as observed in [1].

If the fiber can support several modes with a fixed value of the index m, an incident LG_q^l beam with $l = m$ can couple to all of the modes. To study whether the excitation of a particular fiber mode could be possible in such a case, we use the fiber parameters shown in Table 1, where the wavelength $\lambda = 780$ nm is taken to correspond to the guiding of Rb atoms. Figure 3(a) shows the radial intensity profiles of the $\mathrm{LP}_{m,p}$ modes supported by the chosen fiber. When l and m are both equal to 0 or 1, there are two modes in the fiber, the $\mathrm{LP}_{m,1}$ and $\mathrm{LP}_{m,2}$ modes, which can be excited by an incident LG_q^l beam. All the modes in Fig. 3(a) are

Table 1
Fiber parameters

Parameter	Symbol	Value
Inner core radius	a	3.5 μm
Outer core radius	b	11 μm
Refractive index of the core	n_1	1.4526
Refractive index difference	Δn	0.0026
Wavelength	λ	780 nm

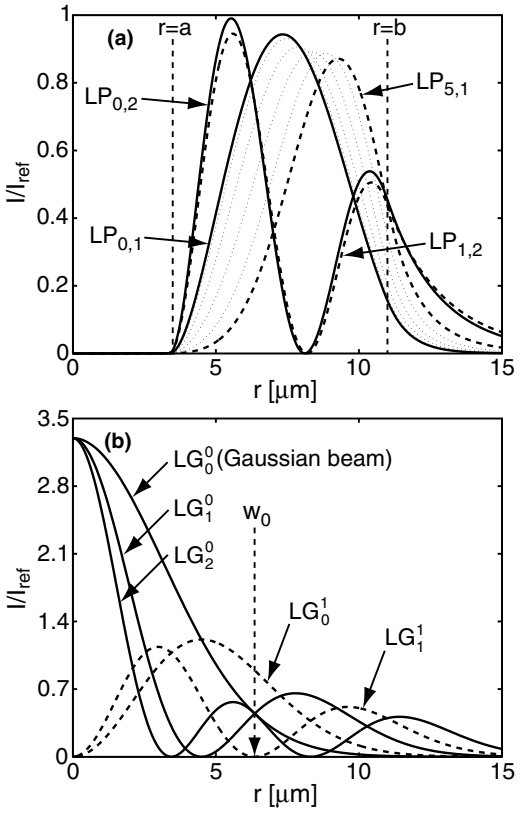

Fig. 3. Radial intensity profiles of: (a) the $LP_{m,p}$ modes in fiber of Table 1; (b) some of the lowest-order LG_q^l beams. All the profiles are normalized with respect to a reference intensity I_{ref} so that the power in each field in (a) and (b) is the same.

normalized to carry the same power. The profiles of the $LP_{0,1}$ and $LP_{0,2}$ modes are plotted with solid lines and the $LP_{5,1}$ and $LP_{1,2}$ modes, having the highest possible values of m, with dashed lines. The two vertical lines mark the inner and outer edges of the fiber core. The relative intensity of a mode on the fiber's inner surface at $r = a$ is highest for the $LP_{0,2}$ mode, and lowest for the $LP_{5,1}$ mode. In Fig. 3(b), we plot the radial intensity profiles of a few LG_q^l beams that have $l = 0$ (solid line) and $l = 1$ (dashed line), which are obtained from Eq. (2) by setting $z' = 0$. The parameter w_0 is set to be the same (see the figure) for each beam, and the beams are all normalized to carry the same power as the individual fiber modes in Fig. 3(a).

To demonstrate how a normal-incidence LG_q^l beam can be used to excite a particular fiber mode, we consider in detail the coupling of an LG_2^0 beam to the modes $LP_{0,1}$ and $LP_{0,2}$. Note that according to Eq. (7), there are no other modes to be excited when the beam is centered at $(x_0, y_0, 0) = (0, 0, 0)$ (see Fig. 2). The excitation coefficients $C_{0,1}$ and $C_{0,2}$ are calculated from Eq. (5) as functions of the parameter w_0 of the beam. By varying w_0, we can in a general case choose which of the $q + 1$ radial extrema of the beam are made to overlap with the p radial extrema of an $LP_{m,p}$ mode (see Figs. 3(a) and 3(b)). By using Eq. (6), we then calculate the intensity $I = |E_{HOF}(a, \theta, z; t)|^2$ on the fiber's inner surface over a 2-cm distance along the z direction and characterize the intensity distribution by finding its mean, maximum and minimum values. The results are illustrated in Fig. 4(a), where the solid, dashed and dash-dotted lines depict the mean, the maximum and the minimum values of intensity in the obtained patterns, respectively. At the points of intersection of the three curves, the intensity distribution is homogeneous, which attributes to the excitation of an individual fiber mode, as indicated in the figure. The most intense of these homogeneous intensity distributions is obtained by setting $w_0 \approx 6.8$ μm to excite the $LP_{0,2}$ mode (the black dot in Fig. 4(a)).

By using the method described above, we have calculated curves similar to those in Fig. 4(a) for a number of incident LG_q^l beams having $l = 0 \ldots 5$. The homogeneous light field of the strongest intensity was then sought for from the intersections of the curves for each beam. These intensities, as well as the corresponding excitation efficiencies $|C_{m,p}|^2$ of the modes, are gathered in Fig. 4(b). In each column separated by the dashed lines, the index q goes from 0 to 3 separately for each value of the index l. The cases, where the excitation of a mode $LP_{m,2}$ takes place are labeled by a line under the black dot. In all other cases, an $LP_{m,1}$ mode is excited. Thus, the leftmost dot in Fig. 4(b) corresponds to the excitation of the $LP_{0,1}$ mode by a Gaussian beam LG_0^0, the next dot to the excitation of the $LP_{0,2}$ mode by an LG_1^0 beam, and so forth. Note that the use of, e.g., an LG_2^0 beam would result in roughly three times as large an intensity as the use of a Gaussian beam. The highest values are seen to originate from the excitation of the $LP_{m,2}$

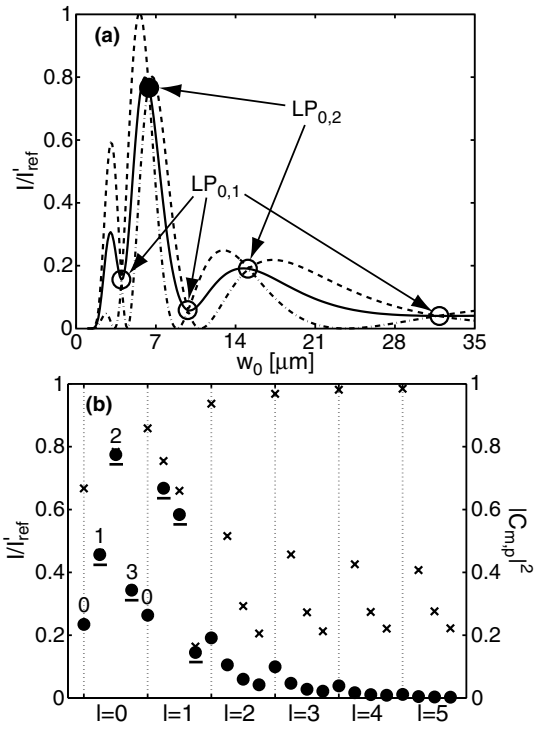

Fig. 4. (a) Mean (solid), maximum (dashed) and minimum (dash-dotted) intensity on the fiber's inner surface resulting from coupling light from an LG_2^0 beam. (b) Maximum intensities obtained by exciting an $LP_{m,1}$ (dot) or an $LP_{m,2}$ mode (underlined dot) by using an LG_q^l beam. The excitation efficiencies $|C_{m,p}|^2$ of the modes are also shown (cross). The index q goes in each column from 0 to 3, which is explicitly shown on the left. The arbitrary reference intensity I'_{ref} is chosen to be the same in (a) and (b).

modes, whereas the excitation efficiency can be very high for a higher-order $LP_{m,1}$ mode.

4. Smoothing the speckle in a multimode fiber

If the total number of modes supported by a HOF is large, the method described in Section 3 is difficult to use in practice. To get rid of the problems caused by a speckled evanescent-wave in such a case, one can use a method mentioned in [10]. The method is based on rapid dithering of the angle of incidence of a beam coupled into the fiber. As a consequence, the intensity profile on the fiber's inner surface changes in time and, if the regions of low and high intensity alternate fast compared to the time an atom spends in the evanescent-wave, the atoms see the field to have a spatially smooth, time-averaged intensity profile. The field will act on the atoms in a similar way as, e.g., the time-averaged orbiting potential (TOP) used in the first observation of Bose–Einstein condensation [16], or as the blue-detuned rotating beam in the ROBOT trap [17].

In the following, we consider the fiber of Table 1 to show how the optimal direction of the dithering and the parameters of the incident Gaussian beam can be obtained to bring about the smoothest possible time-averaged evanescent-wave profile. We assume the beam to be focused onto the fiber core at the point $(x_0, y_0, 0) = ((b+a)/2, 0, 0)$. First, we consider the dithering in the xz plane, i.e., we set $\alpha = 0$ (see Fig. 2). We calculate the evanescent-wave intensity profiles from Eq. (6) for closely-spaced equidistant values of the incident-beam angle $\gamma \in [-NA, NA]$, where NA is the numerical aperture of the fiber. Then, we add up the profiles to obtain an intensity distribution that corresponds to a time-average of the profiles, assuming that the angle γ changes linearly in time. The time-averaged intensity distribution is characterized by the standard deviation σ and the average intensity $\langle I \rangle$ of the pattern over a 2-cm distance along the z direction. The same analysis is applied also for the dithering of the angle α, keeping the angle γ equal to zero. Figure 5 shows the contrast, $C_{\mathrm{sp}} = \sigma/\langle I \rangle$, of the obtained intensity profiles, as well as the contrast of the profile originating from excitation by a normal-incidence beam, as a function of the beam waist w_0. For a completely smooth profile, the contrast C_{sp} would be zero, and if the intensity variations in the profile are large, the contrast will be close to unity. The dithering of the angle α is seen to yield a local minimum for the speckle contrast, while the dithering in the orthogonal direction does not produce such a minimum. The curves approach asymptotically the value corresponding to the dithering of a plane wave, as they should when $w_0 \to \infty$, since the two dithering directions can no longer be distinguished.

The lowest value of the speckle contrast is seen to be about 0.32. We point out that by using fibers

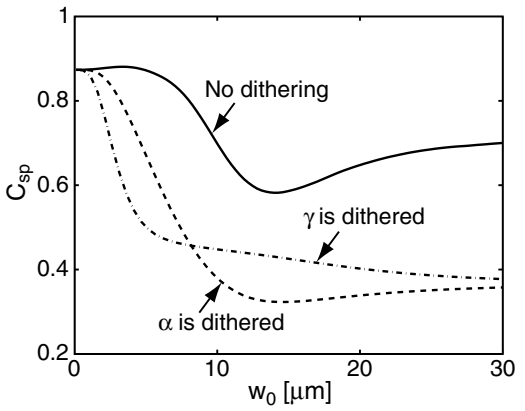

Fig. 5. Contrast in the time-averaged speckle profile as a function of the beam waist in the two dithering directions. Also shown is the contrast when the beam is at normal incidence, i.e., when no dithering is performed.

that support an abundance of modes, the minimum value can be much lower. We have performed similar calculations for multimode fibers supporting up to 26 modes (by keeping the difference $b-a$ constant and describing the modes under the weakly guiding approximation), instead of the 8 modes of the fiber considered above. A local minimum of the speckle contrast C_{sp} was always obtained by dithering the angle α, and the lowest value of about 0.20 was obtained for the fiber supporting the largest amount of modes. The minimum always took place near $w_0 \approx b$, which yields 68% power coupling efficiency from a normal-incidence beam to propagating modes for the fiber of Table 1.

5. Discussion

We have analyzed two methods for obtaining a smooth evanescent-wave profile on the inner surface of a multimode HOF. The first method is based on the excitation of a cylindrical fiber mode with a beam that possesses orbital angular momentum. Laguerre–Gaussian (LG_q^l) beams were considered as examples of such beams. The use of certain higher-order LG_q^l beams was shown to result in roughly a three times as large an evanescent-wave intensity as that resulting from using a Gaussian beam. In the second method, the incident angle of a Gaussian beam coupled to the rim of the fiber core is rapidly dithered. It turned out that the smoothest evanescent-wave profile results from dithering in the direction perpendicular to the plane determined by the fiber axis and the point of excitation, when the beam waist is of the same size as the outer core radius of the fiber.

Depending on the incident-beam parameters in both methods, light can enter the fiber opening. To efficiently load the fiber with atoms, such excess light should be suppressed. In this respect, an LG_q^l beam with $l \neq 0$ would be practical in exciting a particular $\mathrm{LP}_{m,p}$ mode, since such a beam has zero on-axis intensity. On the other hand, the other fiber end can be used for loading of atoms, since the output beams of the $\mathrm{LP}_{m,p}$ modes with $m \neq 0$ are dark on the optical axis [8]. Moreover, the output intensity of each mode is independent of the azimuthal angle, since the output beam and the guided mode have the same azimuthal dependence. Atoms can then be injected into the fiber through the dark central part of a hollow output beam originating from an $\mathrm{LP}_{m,p}$ mode with $m \neq 0$ [13]. In the dithering method, the loading of atoms into the fiber should also be possible from the output end of light, since the contribution of the modes having $m = 0$ to the total field near the fiber axis is rather small, especially in the immediate vicinity of the fiber end.

Acknowledgements

We gratefully acknowledge the financial support by the Academy of Finland. M.H. also acknowledges a grant from the Jenny and Antti Wihuri fund.

References

[1] H. Ito, K. Sakaki, T. Nakata, W. Jhe, M. Ohtsu, Opt. Commun. 115 (1995) 57.
[2] H. Ito, K. Sakaki, T. Nakata, W. Jhe, M. Ohtsu, Ultramicroscopy 61 (1995) 91.
[3] S. Marksteiner, C.M. Savage, P. Zoller, S.L. Rolston, Phys. Rev. A 50 (1994) 2680.

[4] S. Choi, T.J. Eom, J.W. Yu, B.H. Lee, K. Oh, IEEE Photonics Technol. Lett. 14 (2002) 1701.
[5] S. Choi, K. Oh, W. Shin, C.S. Park, U.C. Paek, K.J. Park, Y.C. Chung, G.Y. Kim, Y.G. Lee, IEEE Photonics Technol. Lett. 14 (2002) 248.
[6] R.G. Dall, M.D. Hoogerland, D. Tierney, K.G.H. Baldwin, S.J. Buckman, Appl. Phys. B 74 (2002) 11.
[7] A. Takamizawa, H. Ito, M. Ohtsu, Jpn. J. Appl. Phys. 39 (2000) 6737.
[8] C. Won, S.H. Yoo, K. Oh, U.-C. Paek, W. Jhe, Opt. Commun. 161 (1999) 25.
[9] Y.-I. Shin, M. Heo, J.-W. Kim, W. Shim, H.-R. Noh, W. Jhe, J. Opt. Soc. Am. B: Opt. Phys. 20 (2003) 937.
[10] D. Müller, E.A. Cornell, D.Z. Anderson, E.R.I. Abraham, Phys. Rev. A 61 (2000) 033411.
[11] R.G. Dall, M.D. Hoogerland, K.G.H. Baldwin, S.J. Buckman, J. Opt. B: Quantum Semiclass. Opt. 1 (1999) 396.
[12] M.J. Renn, E.A. Donley, E.A. Cornell, C.E. Wieman, D.Z. Anderson, Phys. Rev. A 53 (1996) R648.
[13] S.H. Yoo, C. Won, J.-A. Kim, K. Kim, U. Shim, K. Oh, U.-C. Paek, W. Jhe, J. Opt. B: Quantum Semiclass. Opt. 1 (1999) 364.
[14] L. Allen, M.W. Beijersbergen, R.J.C. Spreeuw, J.P. Woerdman, Phys. Rev. A 45 (1992) 8185.
[15] J. Courtial, M.J. Padgett, Opt. Commun. 159 (1999) 13.
[16] M.H. Anderson, J.R. Ensher, M.R. Matthews, C.E. Wieman, E.A. Cornell, Science 296 (1995) 198.
[17] N. Friedman, L. Khaykovich, R. Ozeri, N. Davidson, Phys. Rev. A 61 (2000) 031403(R).